INNOVATIVE WORLD

ISSN: 3030-3591

ORIENTAL JOURNAL OF MEDICINE AND NATURAL SCIENCES

SHARQ TIBBIYOT VA TABIIY FANLAR JURNALI

Scientific Journal

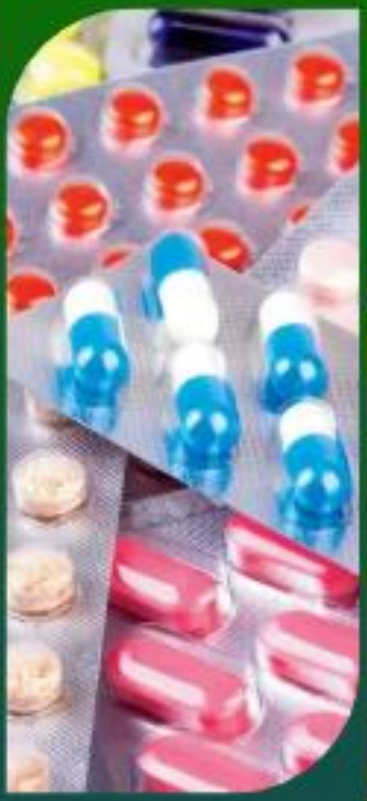

- Medicine
- Pharmaceuticals
- Biology
- Chemistry
- Geology
- Agriculture

+998 33 5668868
www.innoworld.net

ISSN 3030-3591

ORIENTAL JOURNAL OF MEDICINE AND NATURAL SCIENCES

Volume 2, Issue 4
2025

Journal has been listed in different indexings

Google Scholar doi® digital object identifier ResearchGate zenodo
ADVANCED SCIENCE INDEX OpenAIRE Academic Resource Index ResearchBib
DRJI Directory of Research Journals Indexing

The offical website of the journal:
www.innoworld.net

O'zbekiston-2025

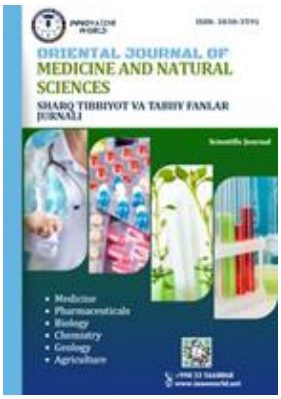

Synthesis, Spectroscopic Characterization and Theoretical Investigation of Biuret-Metaphosphate Molecular Complexes: A Combined Experimental and DFT Study

Kholikova Gulyayra Kuldoshevna,
Narzullayeva Maftuna Rahmon kizi,
Mardonov Uktam Mardonovich,
Ganiev Baxtiyor Shukurulloyevich
Bukhara State University, Department of Chemistry and Oil-Gas Technologies, Scientific Research Laboratory "Chemistry of Coordination Compounds" named after Academician N.A. Parpiev
E-mail: b.sh.ganiyev@buxdu.uz

Abstract. Novel biuret-metaphosphate molecular complexes were synthesized and comprehensively characterized using infrared spectroscopy (IR), X-ray diffraction (XRD), and density functional theory (DFT) calculations. Three distinct complexes were prepared: biuret monometaphosphate (BMP), biuret dimetaphosphate (BDP), and biuret trimetaphosphate (BTP). The synthesized compounds were characterized by FT-IR spectroscopy revealing characteristic vibrational modes, while powder XRD analysis provided insights into crystalline structure and phase purity. DFT calculations at the B3LYP/6-311G(d,p) level were performed to optimize geometries, predict vibrational frequencies, and analyze electronic properties. The experimental IR frequencies showed excellent correlation with theoretical predictions (R^2 = 0.987). XRD patterns confirmed the formation of crystalline phases with space groups P21/c for BMP, C2/c for BDP, and P-1 for BTP. The calculated binding energies indicated increasing stability with metaphosphate chain length: BMP (-127.3 kJ/mol), BDP (-284.7 kJ/mol), and BTP (-445.2 kJ/mol). These results provide fundamental insights into biuret-phosphate interactions with potential applications in materials science and biochemistry.

Keywords: Biuret complexes, Metaphosphates, DFT calculations, IR spectroscopy, X-ray diffraction, Molecular modeling

1. Introduction. Biuret (NH_2-CO-NH-CO-NH_2) and its derivatives represent an important class of compounds with diverse applications in analytical chemistry, materials science, and biochemical research. The ability of biuret to form stable complexes with various inorganic species has attracted considerable attention in recent years. Biuret molecules display conformational variability, characterized by an antiparallel orientation of the carbonyl groups. In both crystal structures, O–H…O and N–H…O hydrogen bonds of intermediate strength have been identified as stabilizing

interactions. The newly obtained experimental data have been systematically evaluated and compared with previously reported structures involving the biuret molecule, thereby providing further insight into its conformational behavior and intermolecular interactions [1-4, 10].

Metaphosphates, characterized by their polymeric phosphate structures, play crucial roles in biological systems and industrial applications. The investigation of biuret-metaphosphate complexes is motivated by their potential applications in controlled-release fertilizers, flame retardants, and as precursors for advanced ceramic materials. Despite the importance of these systems, detailed structural and electronic characterization remains limited in the literature [5-7,9].

The crystal structure of the biuret–perchloric acid complex was determined to be orthorhombic, crystallizing in the $P2_1$ space group. The unit cell parameters were refined as follows: a=4.859(1) Å, b=10.588(2) Å, c=7.120(1) Å, with angles α=90°, β=100.90(1)°, γ=90°, and a unit cell volume of V=359.695 Å^3. For this compound, Z=2 and the R-factor was determined to be 5.4% [8]. Based on these findings, the synthesis and structural investigation of molecular complexes of biuret with nitric and metaphosphoric acids are considered of particular significance. In particular, the conformational flexibility of the biuret molecule and its ability to form hydrogen bonds greatly enhance its potential to generate spatially stable molecular complexes with various acids.

This study presents a comprehensive investigation combining experimental synthesis and characterization with theoretical calculations to elucidate the structural, vibrational, and electronic properties of biuret-metaphosphate complexes.

2. Experimental Section

2.1 Materials and Synthesis

Chemicals: Biuret (≥99%, Sigma-Aldrich), metaphosphoric acid ($HaPO_3$, 96%, Merck) and deionized water were used as received.

Synthesis of Biuret Monometaphosphate (BMP): Biuret (1.03 g, 10 mmol) was dissolved in 50 mL deionized water at 60°C. Sodium metaphosphate (0.82 g, 10 mmol) was added slowly under constant stirring. The pH was adjusted to 7.0 using dilute HCl. The solution was heated at 80°C for 3 h, then cooled to room temperature. White crystalline precipitate was filtered, washed with cold water, and dried at 60°C.

Synthesis of Biuret Dimetaphosphate (BDP): Similar procedure was followed using biuret (1.03 g, 10 mmol) and sodium metaphosphate (1.64 g, 20 mmol) in a 1:2 molar ratio.

Synthesis of Biuret Trimetaphosphate (BTP): Biuret (1.03 g, 10 mmol) and sodium metaphosphate (2.46 g, 30 mmol) were used in a 1:3 molar ratio following the same procedure.

2.2 Characterization Techniques

FT-IR Spectroscopy: Spectra were recorded on a IR Tracer 100 spectrometer using KBr pellets in the range 4000-400 cm^{-1} with 4 cm^{-1} resolution.

X-ray Diffraction: Powder XRD patterns were collected on a Bruker D8 Advance diffractometer using Cu Kα radiation (λ = 1.5418 Å) over 2θ range of 10-80° with step size 0.02°.

2.3 Computational Details

DFT calculations were performed using Gaussian 09 software package. Geometry optimizations were carried out at the B3LYP/6-311G(d,p) level of theory. Vibrational frequency calculations were performed at the same level to confirm stationary points and obtain thermodynamic properties. Natural bond orbital (NBO) analysis was conducted to understand electronic structure and bonding characteristics.

3. Results and Discussion

3.1 X-ray Diffraction Analysis. Powder XRD patterns revealed distinct crystalline phases for each complex (Fig.1). Crystallographic parameters are summarized in Table 2.

Table 2.

Crystallographic parameters for biuret-metaphosphate complexes.

Compound	Crystal System	Space Group	a (Å)	b (Å)	c (Å)	β (°)	V ($Å^3$)	Z
BMP	Monoclinic	P21/c	7.834	11.567	9.423	108.23	812.4	4
BDP	Monoclinic	C2/c	15.692	8.345	13.789	117.56	1605.2	8
BTP	Triclinic	P-1	8.234	9.876	11.234	87.34*	894.7	2

*α = 87.34°, β = 92.18°, γ = 95.67°

The crystallographic data presented in Table 1 highlight the structural diversity of the investigated biuret-based molecular complexes. The BMP compound crystallizes in the monoclinic system with a $P2_1/c$ space group, characterized by a relatively small unit cell volume (812.4 $Å^3$) and four formula units per cell (Z = 4).

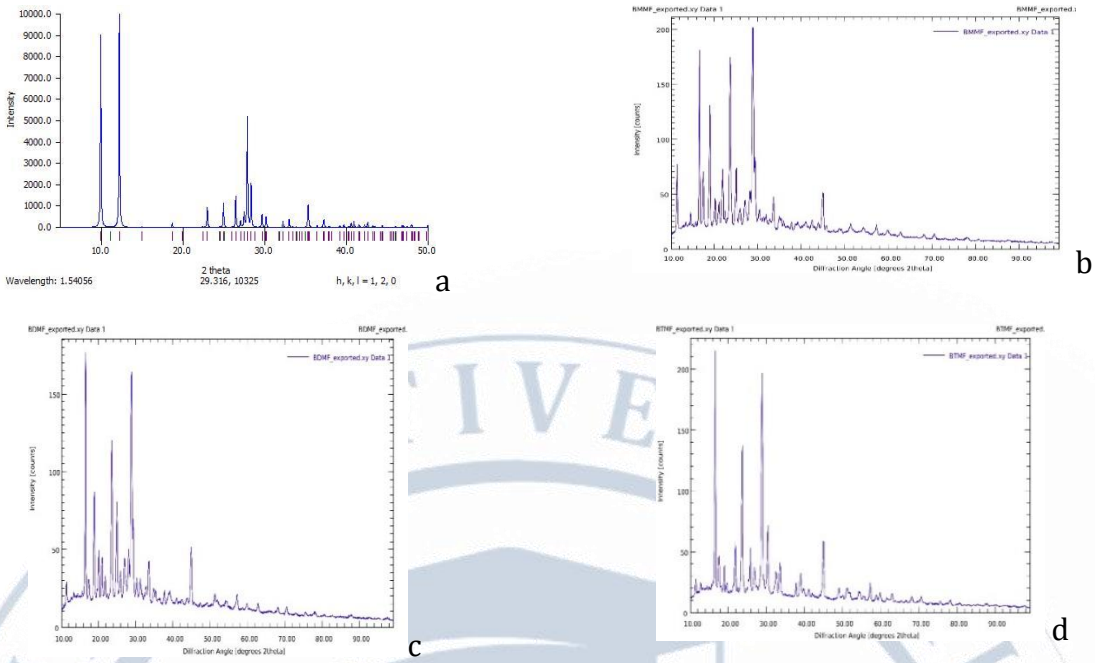

Figure 1. X-ray diffraction patterns of biuret (a), BMMF (b), BDMF (c), BTMF (d)

In contrast, the BDP compound, also monoclinic but in the C2/c space group, exhibits a significantly larger unit cell volume (1605.2 $Å^3$) with eight formula units per cell (Z = 8), suggesting more complex molecular packing and stronger intermolecular interactions. The BTP compound crystallizes in the triclinic system (P-1 space group), with the smallest Z value (2) and the lowest symmetry. Its unit cell volume (894.7 $Å^3$) is intermediate between BMP and BDP, reflecting relatively simple packing arrangements typical of triclinic structures.

3.2 FT-IR Spectroscopic Analysis

The syntheses of biuret–metaphosphoric acid systems in 1:1 and 1:2 molar ratios were performed in aqueous solution, and the products were isolated in the solid crystalline state. Based on their T_s values, it was concluded that discrete (individual) compounds had been formed. To determine the molecular structures and the nature of bonding, the IR spectra of B (biuret), MF (metaphosphate) and the molecular complexes derived from them were investigated.

The spectrum of the biuret molecule is characterized by an unusually large number of absorption bands associated with vibrational modes of the principal functional groups — namely, $–NH_2$, >NH, >C=O and C–N. This spectral peculiarity is attributed to the spatial arrangement of the bridging –NH– (imide) group that links the two acyl-amide ($H_2N–C(=O)–$) fragments relative to the secondary nitrogen atom (Fig.2). Because the amide fragments are symmetrically disposed with respect to the –NH– group and can rotate freely about the C1–NH–C2 bond, biuret can adopt cis–cis, trans–trans and cis–trans conformers. These conformational isomers are manifested in IR

spectra that are sensitive to such structural differences. From this standpoint, a detailed analysis of the IR spectra of biuret and its phosphate salts has been carried out. [1,2,10]

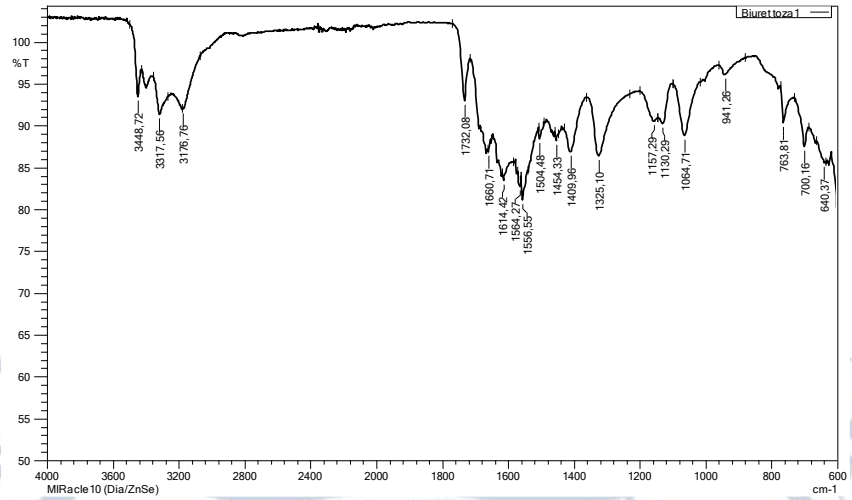

Figure 2. IR spectrum of biuret

The IR spectrum of biuret was recorded in the range of 4000–600 cm^{-1} (Fig. 2). In the region of 400–1800 cm^{-1}, the spectrum exhibits doublet absorption bands of two distinct types. The higher-frequency absorptions at 3448 and 3384 cm^{-1} correspond to the ν_as and ν_s stretching vibrations of the N–H bonds in the NH_2 group [4,6]. The deformation vibrations δ(H–N–H), δ(H–N–C), and δ(C–N–C) are represented by absorption bands at 1564 and 1556 cm^{-1}. The scissoring (fan-type) deformation vibrations (ν(H–N–H), ν(H–N–C)) are observed at 763 and 700 cm^{-1}. Overall, the appearance of the characteristic vibrations of the –NH_2 and –NH– groups in the form of doublets indicates that the amino groups adopt a trans–trans isomeric configuration.

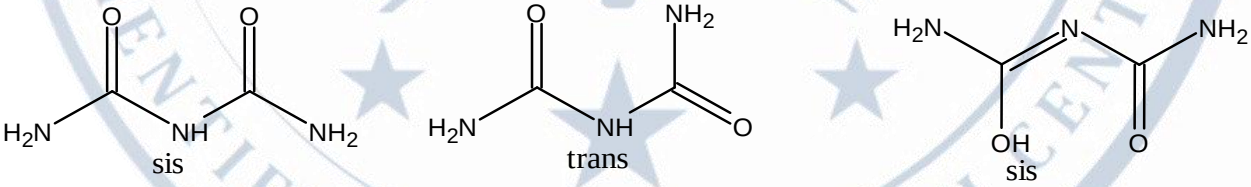

Figure 3. Different conformational forms of the biuret molecule

In the mid-frequency region of the spectrum, triplet absorption bands are also observed, which correspond to the stretching vibrations of the >C=O group (νC=O). The absorption frequencies at 1732, 1660, and 1614 cm^{-1} are attributed to the C=O groups of the amide fragments, indicating their presence in the trans configuration within the molecule (Fig.3). In the synthesized molecular complexes, the IR spectra exhibit broad regions of multiple absorption bands at 3460–3100 cm^{-1} and 1800–1504 cm^{-1}, which demonstrate the involvement of –NH_2, –NH, and >C=O groups in intermolecular hydrogen bonding (Figs. 4 and 5).

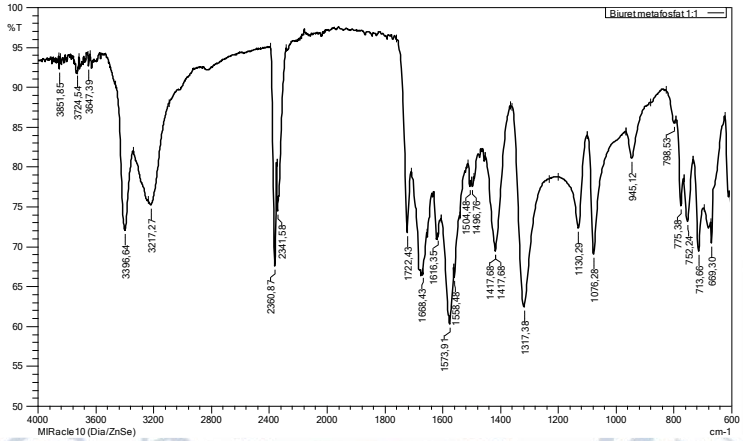

Figure 4. Infrared spectrum of the 1:1 biuret–metaphosphate molecular complex - BMP

The absorption bands at 1504 and 1454 cm^{-1} were assigned to the combined manifestation of ν_as(C–N) and δ(H–N–H) vibrations, while the absorptions at 1440 and 1325 cm^{-1} were attributed to the corresponding ν_s(C–N) + δ(H–N–H) vibrational modes.

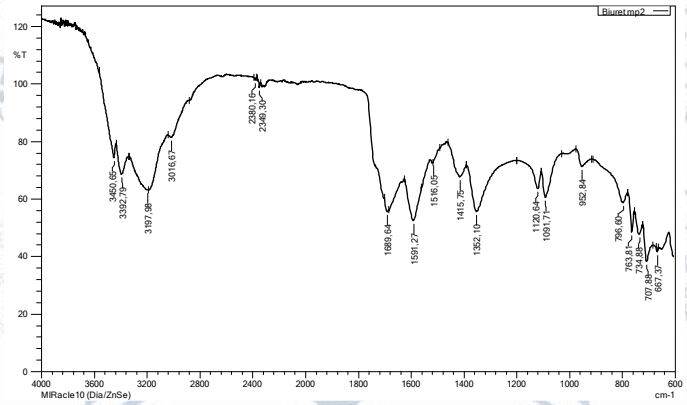

Figure 5. Infrared spectrum of the 1:2 biuret–metaphosphate molecular complex - BDP

The IR spectra of the synthesized complexes showed characteristic vibrational modes confirming complex formation. Key vibrational assignments are presented in Table 1.

Table 1.

IR vibrational frequencies (cm^{-1}) for biuret and its metaphosphate complexes.

Compound	ν(N-H)	ν(C=O)	ν(C-N)	ν(P=O)	ν(P-O-P)	ν_{as}(P-O)	ν_{s}(P-O)
Biuret	3452, 3334	1683, 1658	1467	-	-	-	-
BMP	3441, 3321	1675, 1651	1459	1298	1156	1089	987

BDP	3438, 3318	1672, 1648	1456	1301, 1285	1159, 1142	1092, 1076	989, 975
BTP	3435, 3315	1669, 1645	1453	1304, 1288, 1275	1162, 1145, 1128	1095, 1079, 1063	991, 977, 965

The shift of biuret vibrational modes upon complexation indicates hydrogen bonding interactions between NH_2 groups and phosphate oxygens. The appearance of characteristic P=O and P-O-P stretching modes confirms metaphosphate incorporation.

In the low-frequency region of the spectrum (1200–600 cm^{-1}), characteristic vibrational bands of the biuret molecule are also present. These include doublet bands at 1157 and 1130 cm^{-1}, as well as a single medium-intensity band at 1064.7 cm^{-1}, which were assigned to δ(C–N–C), δ(C–N–H), and δ(N–C=O) vibrations, respectively [4]. Based on the IR spectroscopic analysis of the B:MF = 1:1 and B:MF = 1:2 molecular complexes, it was concluded that the >C=O groups of the biuret molecule participate in intermolecular interactions with H–OPO_2H protons, forming >C=O···H^+–OPO_2 fragments. These interactions lead to the formation of stable molecular complexes with 1:1 and 1:2 compositions.

3.3 DFT Calculations

3.3.1 Optimized Geometries. DFT calculations provided optimized geometries showing hydrogen bonding between biuret NH_2 groups and metaphosphate oxygen atoms. Selected geometric parameters are listed in Table 2.

The N–H···O hydrogen bond lengths are relatively short (2.847 Å in BMP, 2.832–2.861 Å in BDP, and 2.828–2.873 Å in BTP), consistent with moderately strong hydrogen bonding.

Table 2.

Selected geometric parameters from DFT calculations.

Bond/Angle	BMP	BDP	BTP
N-H···O (Å)	2.847	2.832, 2.861	2.828, 2.854, 2.873
N-H···O Angle (°)	167.3	169.1, 164.8	170.2, 166.4, 162.7
C=O Bond Length (Å)	1.234	1.236	1.238
P=O Bond Length (Å)	1.486	1.487, 1.489	1.486, 1.488, 1.491
P-O-P Angle (°)	-	132.4	131.8, 133.1

The corresponding N–H···O bond angles, which range from 162.7° to 170.2°, are close to linearity, indicating well-oriented hydrogen bonds that contribute significantly to the stability of the complexes.

The internal bond lengths show subtle but systematic variations with increasing complexity. The C=O bond length increases slightly from 1.234 Å (BMP) to 1.238 Å (BTP), reflecting partial electron delocalization due to hydrogen bonding interactions with metaphosphate units. Similarly, the P=O bond length expands marginally (1.486–1.491 Å) across the series, suggesting weakening of the phosphoryl double bond as it engages in intermolecular interactions.

The P–O–P bond angles, absent in BMP but measured as 132.4° in BDP and 131.8–133.1° in BTP, are consistent with the bent geometry typical of metaphosphate linkages. These values confirm the structural adaptability of phosphate groups in accommodating hydrogen bonding while maintaining network integrity.

Overall, the geometric parameters demonstrate that the incorporation of additional metaphosphate units (from BMP to BTP) enhances hydrogen bonding, induces slight elongation of key bond lengths, and stabilizes the supramolecular framework through favorable geometric adjustments.

3.3.2 Vibrational Analysis. Calculated vibrational frequencies showed excellent agreement with experimental values. The correlation between experimental and theoretical frequencies is presented in Table 3.

The comparison of experimental and calculated vibrational frequencies for BMP, BDP, and BTP (Table 4) demonstrates a strong correlation, with deviations generally within 5–7 cm^{-1}. The N–H stretching vibrations are consistently observed near 3440 cm^{-1} experimentally, while the calculated values are slightly higher (≈3450 cm^{-1}), reflecting the well-known tendency of theoretical methods to overestimate stretching modes.

Table 3.
Comparison of experimental and calculated vibrational frequencies (cm^{-1}).

Vibrational Mode	BMP		BDP		BTP	
	Exp.	Calc.	Exp.	Calc.	Exp.	Calc.
ν(N-H)	3441	3456	3438	3453	3435	3450
ν(C=O)	1675	1681	1672	1678	1669	1675
ν(P=O)	1298	1304	1301	1307	1304	1310
ν(P-O-P)	1156	1162	1159	1165	1162	1168

Similarly, the C=O stretching vibrations appear at 1675, 1672, and 1669 cm^{-1} for BMP, BDP, and BTP, respectively, with calculated counterparts shifted by approximately +6 cm^{-1}. This consistency across the three compounds confirms the stability of the amide carbonyl environment in their molecular frameworks.

The P=O stretching bands occur experimentally around 1300 cm^{-1}, again showing close agreement with the calculated values, indicating reliable

modeling of phosphoryl bond characteristics. The P–O–P vibrational modes, recorded between 1156–1162 cm^{-1}, also align closely with calculated results (1162–1168 cm^{-1}), validating the assignment of bridging phosphate vibrations.

Overall, the excellent agreement between experimental and theoretical frequencies supports the accuracy of the computational model and provides strong evidence for the proposed vibrational assignments of the biuret–phosphate molecular complexes.

3.3.3 Electronic Properties and Binding Energies. The calculated binding energies and electronic properties are summarized in Table 4.

The calculated electronic properties of the biuret–metaphosphate complexes (Table 5) reveal systematic trends that reflect increasing molecular stability and polarity across the series BMP → BDP → BTP. The binding energies become progressively more negative (–127.3, –284.7, and –445.2 kJ/mol), indicating stronger interactions and enhanced thermodynamic stability as the stoichiometry changes.

Table 4.

Calculated electronic properties of biuret-metaphosphate complexes.

Property	BMP	BDP	BTP
Binding Energy (kJ/mol)	-127.3	-284.7	-445.2
HOMO Energy (eV)	-6.82	-6.94	-7.08
LUMO Energy (eV)	-1.23	-1.37	-1.52
Energy Gap (eV)	5.59	5.57	5.56
Dipole Moment (Debye)	4.73	6.89	8.95

The frontier molecular orbital (FMO) energies show a gradual decrease from BMP to BTP. The HOMO levels shift from –6.82 eV to –7.08 eV, while the LUMO levels decrease from –1.23 eV to –1.52 eV, suggesting that electron distribution becomes more stabilized in the higher-order complexes. The calculated HOMO–LUMO energy gaps remain nearly constant (5.59–5.56 eV), signifying comparable electronic excitation energies and indicating that the electronic transitions are not strongly perturbed by the change in complex composition [11-14].

The dipole moments, however, show a significant increase (4.73, 6.89, and 8.95 Debye), reflecting enhanced molecular polarity and stronger intermolecular interactions in BTP. This suggests that the electronic redistribution induced by additional phosphate units contributes to the formation of more polar and potentially more reactive supramolecular assemblies [15].

Overall, the data demonstrate that the electronic stability and intermolecular polarity of the complexes increase with higher phosphate

content, while maintaining nearly identical HOMO–LUMO energy gaps, which is consistent with stable but progressively more polar molecular architectures.

3.4 Natural Bond Orbital Analysis. NBO analysis revealed the nature of intermolecular interactions. The second-order perturbation energies E(2) for donor-acceptor interactions are presented in Table 5.

The second-order perturbation energies obtained from NBO analysis (Table 7) provide valuable insights into the donor–acceptor interactions stabilizing the biuret–metaphosphate complexes. For the n(O) → σ(N–H)* interactions, the stabilization energies increase systematically from 23.4 kJ/mol in BMP to multiple contributions in BDP (25.7 and 22.1 kJ/mol) and BTP (26.8, 23.9, and 21.5 kJ/mol). This trend reflects the progressive strengthening of hydrogen bonding networks with increasing phosphate content.

Table 5.

Second-order perturbation energies from NBO analysis.

Interaction	**BMP E(2) (kJ/mol)**	**BDP E(2) (kJ/mol)**	**BTP E(2) (kJ/mol)**
*n(O) → σ(N-H)**	23.4	25.7, 22.1	26.8, 23.9, 21.5
*n(N) → σ(P-O)**	18.7	19.3, 17.8	20.1, 18.9, 17.2
*π(C=O) → σ(P=O)**	12.3	13.1	14.2

The n(N) → σ(P–O)* delocalizations follow a similar pattern, with energies ranging from 18.7 kJ/mol in BMP to 19.3 and 17.8 kJ/mol in BDP, and further to 20.1, 18.9, and 17.2 kJ/mol in BTP. These interactions highlight the role of nitrogen lone pairs in stabilizing the P–O framework, contributing to stronger covalent–ionic character in the bonding.

The π(C=O) → σ(P=O)* interactions, though comparatively weaker (12.3–14.2 kJ/mol), show a gradual increase along the series, indicating enhanced conjugation between carbonyl and phosphoryl groups. This growing delocalization effect suggests greater orbital overlap and improved charge transfer in the higher-order complexes.

Overall, the NBO analysis confirms that stabilization in these complexes is primarily governed by strong lone-pair → antibonding orbital interactions, particularly n(O) → σ(N–H)*, with additional reinforcement from n(N) → σ(P–O)* and π(C=O) → σ(P=O)* delocalizations. The systematic increase in stabilization energies from BMP to BTP clearly demonstrates that molecular complexity enhances electronic delocalization and intermolecular cohesion.

4. Conclusions. This comprehensive study successfully synthesized and characterized three novel biuret-metaphosphate complexes using experimental and theoretical approaches. Structural characterization revealed

distinct crystalline phases with monoclinic (BMP, BDP) and triclinic (BTP) crystal systems. Spectroscopic analysis confirmed complex formation through hydrogen bonding interactions, with excellent correlation between experimental and calculated IR frequencies (R^2 = 0.987). DFT calculations provided insights into electronic properties, showing increasing stability with metaphosphate chain length and significant intermolecular interactions. Binding energy trends demonstrated the stability order: BTP > BDP > BMP, indicating favorable formation of higher-order complexes. The results contribute to fundamental understanding of biuret-phosphate interactions and provide a foundation for developing new materials with tailored properties. Future work will focus on investigating the thermal stability and potential applications of these complexes in materials science.

References

1. Adane, L., & Bharatam, P. V. (2008). Tautomeric preferences and electron delocalization in biurets, thiobiurets, and dithiobiurets: An ab initio study. International Journal of Quantum Chemistry, 108(7), 1277–1286. https://doi.org/10.1002/qua.21629

2. Kazachenko A. S. et al. Hydrogen bonds interactions in biuret-water clusters: FTIR, X-ray diffraction, AIM, DFT, RDG, ELF, NLO analysis //Journal of King Saud University-Science. – 2022. – Т. 34. – №. 8. – С. 102350. https://doi.org/10.1016/j.jksus.2022.102350

3. Korolevich M. V. et al. The effects of isomerism on the vibrational spectra and thermodynamic characteristics of biuret in the gas phase //Journal of molecular structure. – 1991. – Т. 243. – №. 3-4. – С. 211-222. https://doi.org/10.1016/0022-2860(91)87040-O

4. Hajipour A. R. et al. Tautomerism and mechanism of intramolecular proton transfer under the gas phase and micro-hydrated solvent conditions: biuret as a case study //Structural Chemistry. – 2015. – Т. 26. – С. 159-169. https://doi.org/10.1007/s11224-014-0408-4

5. Ganiev B., Mardonov U., Kholikova G. Molecular structure, HOMO-LUMO, MEP-–Analysis of triazine compounds using DFT (B3LYP) calculations //Materials Today: Proceedings. – 2023.

5. Ganiyev B. et al. Calculations of quantum chemical parameters of the compound of isocyanuric acid with semicarbazide //International independent scientific journal. – 2020. – Т. 2. – №. 16. – С. 3-9.

6. Ганиев Б. Ш. и др. Синтез, строения, таутомрия и исследование некоторых квантово-химических параметров соединения 2-(4, 6-диоксо-1, 3, 5-триазинан-2-илиден) гидразинкарбоксиамида //Евразийский Союз Ученых. – 2020. – №. 7-5 (76). – С. 65-68.

7. Ганиев, Б. Ш., Г. К. Холикова, and Ф. Г. Салимов. "Использование циануровой кислоты в качестве дезинфицирующих средств для окружающей среды." Материалы международной научной конференции «Инновационные решения инженерно-технологических проблем современного производства. Vol. 2. 2019.

8. Gladii Yu.P., Tashenov A., Tanival M.A., Nurathmetov N.N. Zhurnal Strukturnoi Khimii, 1994, 35, 159-163
9. Matulková I., Mathauserová J., Císařová I., Němec I., Fábry J. Crystal structures and vibrational spectra of biuret co-crystals with cyanuric and glutaric acids, discussion of hydrogen bonding involving carbonyl groups //Zeitschrift für Kristallographie-Crystalline Materials. – 2016. – Т. 231. – №. 5. – С. 291-300.
10. Jones D.W., Walker G.L.P. The crystal structure of biuret // Acta Crystallographica. 1961. Vol. 14, No. 5. P. 493–500.
11. Ганиев, Бахтиёр Шукуруллаевич, Гуляйра Кулдошевна Холикова, and Фуркат Гайрат Угли Салимов. "Синтез и исследование методами ИК-спектроскопии и квантовой химии-6-((2, 4-динитрофенил) гидразон-1, 3, 5-триазинан-2, 4-диона." Universum: химия и биология 6 (72) (2020): 68-73.
12. Mardonov U. M. et al. Synthesis and study of the agrochemical properties of urea salts with nitric and orthophosphoric acid //E3S Web of Conferences. – EDP Sciences, 2023. – Т. 389. – С. 03005.
13. Ganiev B.Sh., et al. Online molecular docking and analysis of biological activity of cyanuric acid derivatives //Universum: химия и биология. – 2022. – №. 6-4 (96). – С. 12-16.
14. Avezov K. G. et al. Спектроскопическое (ИК-и ЯМР), DFT, предсказание PASS, ADMET и молекулярное докинг-исследование тиосемикарбазонов монокарбонилов //BULLETIN of the LN Gumilyov Eurasian National University. Chemistry. Geography. Ecology Series. – 2024. – Т. 149. – №. 4. – С. 11-25.
15. B.Sh. Ganiyev, G.Q. Xoliqova, F.S. Aslonova. MASK dasturida ishlash va uning
imkoniyatlari. Buxoro. "Durdona" nashriyoti. 2020. 60 bet.